Magnetospheric Electric Fields and Their Variation with Geomagnetic Activity

MARGARET GALLAND KIVELSON

Department of Geophysics and Space Physics and Institute of Geophysics and Planetary Physics
University of California, Los Angeles, California 90024

Diverse and independent measurements of the variation of particle convection boundaries with geomagnetic activity are used to obtain relations between the magnitude of a large scale electric field and the *Kp* index. The relations are compared with measured fields and with models and are found to be consistent with diverse observations and probably more reliable than results previously obtained.

INTRODUCTION

The importance of large scale electric fields in the dynamics of the magnetosphere has been emphasized both in broad reviews [*Axford*, 1969; *Vasyliunas*, 1970*a*; *Chappell*, 1974; *Stern*, 1975] and in more specialized studies [*Kavanagh et al.*, 1968; *Chen*, 1970; *Mozer*, 1971; *Rycroft*, 1971; *Volland*, 1973; *Mozer and Lucht*, 1974]. These studies conclude that satisfactory qualitative interpretations of varied aspects of magnetospheric dynamics such as particle injection and acceleration, low-energy plasma convection, and the motion of whistler ducts emerge from analysis of the response to simple analytic representations of large scale electric fields. It is apparent, however, that more detailed understanding of the effects of electric fields on particle behavior requires field models of greater complexity, models which provide for localized spatial effects [for example, *Wolf*, 1970; *McIlwain*, 1974], and models which, though still static, vary in an empirically established way with the level of geomagnetic activity [*Vasyliunas*, 1968; *Rycroft*, 1971; *Chen and Grebowsky*, 1974; *Maynard and Chen*, 1975]. The present paper addresses the latter problem, obtaining a relation between the magnitude of a uniform cross-magnetosphere electric field and the *Kp* index which is compatible with diverse and independent measurements of particle boundaries in different local time regions of the magnetosphere and therefore probably more reliable than results previously obtained.

In this paper the comparisons with both theory and observation stress local times other than dusk. This emphasis is based on the argument that the quasi-steady state convection model alone is not likely to describe phenomena near the stagnation point where the convection electric field is counteracted by the corotation electric field. The large scale electric fields in this region may be small with respect to localized and time-varying electric fields. The action of localized and time-varying fields may prevent the plasma from reaching equilibrium in the combined convection and corotation fields in the 'bulge' region near dusk.

Correlations between various interplanetary and magnetospheric parameters and the *Kp* index have been noted in the past, and though the correlations are crude, they help illuminate the underlying physical processes. For example, *Snyder et al.* [1963] and *Vasyliunas* [1968] have related *Kp* to the solar wind velocity, *Wilcox et al.* [1967] and *Schatten and Wilcox* [1967] have related it to the magnitude of the interplanetary magnetic field, numerous workers have expressed the distance to the plasmapause in terms of this parameter [*Carpenter*, 1967; *Binsack*, 1967; *Taylor et al.*, 1968; *Bezrukikh*, 1970; *Chappell et al.*, 1970*a*; *Rycroft and Thomas*, 1970], and, more recently, *Mauk and McIlwain* [1974] and *Freeman* [1974] have expressed the local time at which substorm-injected low-energy particles are observed by a geostationary satellite in terms of *Kp*. Analogous correlations for low-altitude phenomena include the dependence of the auroral zone boundaries on *Kp* and closely related indices [*Feldstein and Starkov*, 1967; *Feldstein*, 1972, 1974] and the dependence of ionospheric electric field magnitudes on *Kp* [*Mozer and Lucht*, 1974]. By inference from relations discussed above, *Vasyliunas* [1968] and *Mendillo and Papagiannis* [1971] have inferred relations between the solar wind velocity and the magnetospheric electric field, and *Freeman* [1974] has inferred the distance to the inner edge of the plasma sheet at midnight as a function of *Kp*. In the next section, the *Kp* dependences of convection boundaries in the equatorial plane are used to obtain empirical relations between *Kp* and the magnitude of a uniform dawn-dusk electric field, *E*. The results obtained are compared with independent measurements of the total potential drop across the polar cap [*Heppner*, 1972] and with low-altitude properties. Results based on a uniform cross-magnetosphere field are compared with those based on more sophisticated models [*Volland*, 1973; *McIlwain*, 1974; *Stern*, 1975; *Maynard and Chen*, 1975], and differences are not large for small *Kp*. Observations of the plasmapause during a geomagnetic storm [*Hoffman et al.*, 1975] show that the relation obtained is consistent with observations even at very large *Kp*. In the final section, a relation between solar wind velocity and *Kp* is given, and properties of the inner edge of the plasma sheet at midnight are evaluated.

E VERSUS *Kp*, FROM EQUATORIAL CONVECTION BOUNDARIES

In the presence of a dawn-dusk electric field the drift orbits of low-energy charged particles which completely encircle the earth lie inside a boundary called the Alfvén layer [*Schield et al.*, 1969]. (Particle orbits and Alfvén layers in a uniform dawn-dusk field have been discussed by *Alfvén and Fälthammar* [1963], *Kavanagh et al.* [1968], *Schield* [1969], *Chen* [1970], and *Kivelson and Southwood* [1975].) *Nishida* [1966] and *Brice* [1967] recognized that this outermost closed drift orbit (or, equivalently, the last closed equipotential) would, in a static situation, correspond to the plasmapause. Experimentally, the plasmapause must be defined as the outermost sustained closed equipotential contour [*Carpenter and Park*, 1973; *Chen and Grebowsky*, 1974]. The requirement that a field configuration be sustained arises for somewhat different reasons when the field increases than when it decreases. In the case of a field increase, filled flux tubes on newly open orbits continue to drift around the earth until they reach the late afternoon quadrant, where they drift out toward the magnetopause. As it takes ~1 day for plasma initially in the evening sector to move away from the Alfvén layer, the new equilibrium plasmapause position is achieved only after ~1 day. For this reason, in some parts of this paper the average *Kp* for the previous 24 hours is used to characterize the magnetic conditions. On the other hand, freshly injected particles on orbits open to the tail appear at the new Alfvén boundary in the evening-midnight quadrant within hours of the increase in the convection field; hence, in the interpretations based on night side injection boundaries, the *Kp* index for the time of observation is used. In the case of a decreasing field, flux tubes on newly closed orbits refill completely only after 5–8 days [*Park,* 1970]. For this reason the Alfvén boundary based on the 24-hour *Kp* may not correspond to the plasmapause during intervals of decreasing activity.

Inward displacement of the plasmapause with increasing magnetic activity [*Carpenter,* 1967; *Rycroft and Thomas,* 1970] is consistent with the existence of a *Kp*-related dawn-dusk electric field across the magnetosphere, as noted by *Rycroft* [1974]. For the earth's dipole magnetic field the position of the Alfvén layer in a uniform dawn-dusk electric field is found from the equations

$$-eER_E L(\phi) \sin \phi + C/L(\phi) = eER_E L_s + C/L_s \quad (1a)$$

$$eER_E L_s = C/L_s \quad (1b)$$

[*Kivelson and Southwood,* 1975], where $L(\phi)$ is the radial distance (in earth radii) to the Alfvén layer in the equatorial plane at azimuth ϕ (ϕ measured eastward from midnight), $C = e\Omega B_0 R_E^2 \simeq 90$ keV with $\Omega = 2\pi$/day, and B_0 the equatorial field strength at 1 R_E; L_s is the distance to the flow stagnation point on the dusk meridian, and E is the magnitude of the dawn-dusk electric field in the equatorial plane (in kV R_E^{-1}). Equations (1*a*) and (1*b*) can be manipulated to show that $L(\phi)$ and E are related by

$$L^2(\phi)eER_E = C\{[1 - (1 + \sin \phi)^{1/2}]/\sin \phi\}^2 \quad (2)$$

The azimuthal variation (or local time dependence) of the distance to the boundary given by (2) has been shown by *Rycroft* [1971] to agree well with observations from 2100 LT through dawn to noon.

Equation (2) can be used in conjunction with one of the empirical relations between *Kp* and the distance to the plasmapause to yield a relation between *E* and *Kp*. For example, *Carpenter* [1967], using whistlers to determine the distance to the plasmapause near dawn ($L_D = L(90°)$), found a linear relation between L_D and the highest 3-hour *Kp* index in the 24 hours preceding his measurement. Using the fit to this observation [*Carpenter and Park,* 1973]

$$L_D \simeq 5.7 - 0.47Kp \qquad Kp \leq 6 \quad (3)$$

with (2), we find

$$E = 0.46/(1 - 0.082Kp)^2 \ \ \text{kV}/R_E \quad (4)$$

This relation is relatively insensitive to the local time assigned to (3), which is based on measurements in the midnight-dawn sector. For example, if (3) is taken to represent $L(45°)$, the field of (4) increases by 10%.

As the empirical relations between the plasmapause distance and *Kp* obtained by *Binsack* [1967], *Bezrukikh* [1970], *Gringauz* [1969], *Chappell et al.* [1970*a*], and *Rycroft and Thomas* [1970] are quite similar to that of *Carpenter* [1967] (see the discussion in the review of *Rycroft* [1975]), (4) can be considered representative of the relations which follow from this type of measurement. The functional form of (4) is partially a consequence of the use of a linear fit to the plasmapause observations. A different form follows from the empirical relation for L_{pp}, the distance to the plasmapause at night

$$L_{pp} = 5.64 - (0.78 \pm 0.12)(Kp)^{1/2} \qquad Kp \leq 6 \quad (5)$$

which *Rycroft and Thomas* [1970] reported as an improvement over the linear fit to their data. As their measurements were made at night, we set $\phi = 0$ in (2) to obtain

$$E = 0.71/[1 - 0.14(Kp)^{1/2}]^2 \ \ \text{kV}/R_E \quad (6)$$

Equation (6) gives $E = 0.71$ and 1.44 kV/R_E for $Kp = 0$ and 5^-, respectively, as noted by *Rycroft* [1974], but the dependence differs slightly from the linear one he mentions. Equations (4) and (6) are plotted in Figure 1. Also plotted in Figure 1 are two points relating *E* and *Kp* obtained by *Rycroft* [1971] from considerations of the local time asymmetry of the plasmapause.

A relation between *E* and *Kp* which agrees well with the results of the plasmapause analysis (equation (4)) can be obtained from an analogous treatment of the observations of the local time of injection of substorm-associated particles at geostationary orbit. *Mauk and McIlwain* [1974] and *Freeman* [1974] found there is an approximately linear relation between *Kp* and the local time, primarily between dusk and midnight, at which freshly injected particles are encountered. Their observations are shown in Figures 2*a* and 2*b*. Low-energy particles, injected in the premidnight region by a cross-magnetosphere electric field associated with a substorm, must be on drift orbits open to the geomagnetic tail [*Kivelson and Southwood,* 1975]; that is, they must be outside their Alfvén layer $L(\phi)$, specified by (2). This boundary is plotted in Figure

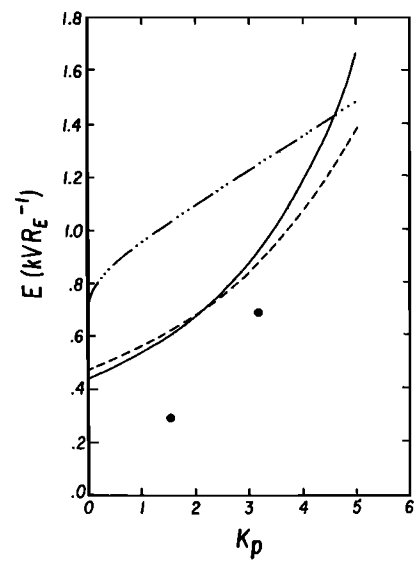

Fig. 1. Magnitude of a uniform dawn-dusk electric field versus *Kp*. The dashed line represents data inferred from *Carpenter*'s [1967] measurements of equatorial distance to the dawn plasmapause (equation (4)). The solid line is data inferred from *Mauk and McIlwain*'s [1974] measurements of the low-energy particle injection boundary (equation (11)). The dotted and dashed line represents data inferred from *Rycroft and Thomas*'s [1970] measurements of distance to night side plasmapause (equation (6)). The two points were found by *Rycroft* [1971] from studies of the local time dependence of the plasmapause.

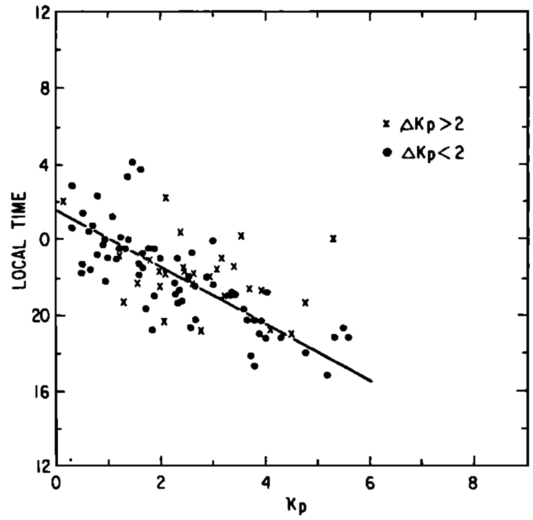

Fig. 2*a*. The local time of low-energy particle injection at geostationary orbit by *Mauk and McIlwain* [1974], (8).

3 for a number of different values of E. Also shown is the approximate orbit of a geostationary satellite; no corrections have been made for dipole tilt. From the figure it is apparent that in the late evening quadrant the satellite crosses the boundary at local times which are earlier the greater the strength of the electric field. From (2), with $L(\phi) = 6.6$, we obtain

$$E = 2.1\{[1 - (1 + \sin\phi)^{1/2}]/\sin\phi]\}^2 \quad kV/R_E$$
$$E = 2.1/\{1 + 2^{1/2}\ |\cos[(\phi - 90°)/2]|\}^2 \quad kV/R_E \qquad (7)$$

as the relation between the local time (ϕ) at which the first freshly injected particles should appear at geostationary orbit and the strength of the dawn-dusk electric field. Equation (7) can be used in conjunction with either of the relations between local time of encounter and Kp:

$$LT = \phi/15° = 25.5 - 1.5Kp \qquad Kp \leq 5^+ \qquad (8)$$

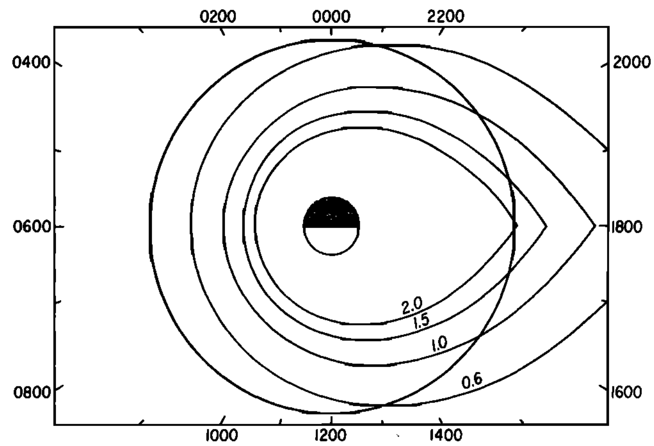

Fig. 3. Zero energy Alfvén layers in the equatorial plane for different magnitudes of a uniform dawn-dusk electric field. The boundaries are labelled with the values of E in kV R_E^{-1}, and the orbit of a geostationary satellite is shown as a circle. In the evening quadrant the intersection of the satellite with the Alfvén layer is seen to occur at later local times for smaller values of E.

[*Mauk and McIlwain*, 1974] or

$$LT = 27.6 - 1.6Kp \qquad Kp \leq 8^- \qquad (9)$$

[*Freeman*, 1974] to obtain a relation between E and Kp.

As the naturally occurring time variable in the model is sin ϕ, and the time variable in terms of which E is most simply expressed is $s = |\cos[(\phi - 90°)/2]|$ (see equation (7)), we could obtain an algebraic relation between E and Kp if Kp were correlated with s instead of LT. Accordingly, we have found the least square fit to s as a function of Kp from the data of Mauk and McIlwain. Having verified that our data set closely reproduces their fit ($LT = 25.3 - 1.42Kp$, standard deviation: 1.58), we obtained a fit for s versus Kp

$$s = 0.825 - 0.148Kp \qquad (10)$$

The standard deviation for this fit shows it to be comparable to

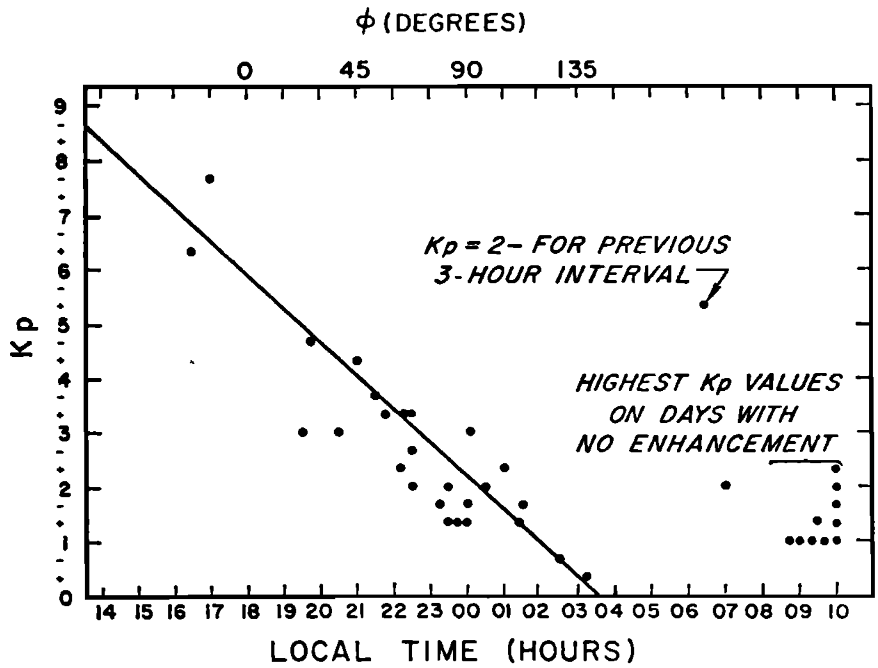

Fig. 2*b*. The local time of low-energy particle injection at geostationary orbit by *Freeman* [1974], (9).

the fit for LT versus Kp. From (7) and (10), we then find (see Figure 1)

$$E = 0.44/[(1 - 0.097Kp)^2] \quad kV/R_E \qquad (11)$$

Analogous treatment of Freeman's data is not useful unless his two points at $Kp > 6$ are excluded, because the theoretical model cannot predict the local time of injection if the electric field is large enough to move the stagnation point inside of geostationary orbit. For the observations at $Kp < 6$ the fit

$$s = 0.954 - 0.141Kp \qquad (12)$$

yields a result similar to that of (4) and (11), i.e.,

$$E = 0.39/[(1 - 0.086Kp)^2] \quad kV/R_E \qquad (13)$$

The electric fields of (11) and (13), deduced from observations of the equatorial convection boundary identified at each local time as the minimum distance to which newly injected low-energy particles penetrate during a substorm, should in a steady state convection model correspond to the field (4) inferred from the location of the equatorial plasmapause identified as the radial distance at which the gradient of cold plasma density increases rapidly with radial distance. Despite the problems discussed in the introduction of identifying the plasmapause in a time-varying situation and despite the fact that the two boundaries are measured in different local time sectors, the three equations are in good agreement over a large range of Kp. For large values of Kp, one might expect the relation found from the plasmapause position to be more dependable than (11) and (13) because the convection boundary, which limits the inward injection observed by a geostationary satellite, lies increasingly close to the 'bulge' region of the plasmapause (see Figure 3) for increasingly large E, and the 'bulge' region is known to be highly variable in structure [*Chappell et al.*, 1970*b*; *Rycroft*, 1975]. For $E \gtrsim 1.5$ kV/R_E, small departures from the assumed symmetry would produce large changes in the local time at which injection was first observed. Inspection of Figure 2*a* suggests that the linear relation between LT and Kp may not be significant for $LT <$ 1800 or for $Kp > 4$. Figure 2*b*, on the other hand, shows that the only two measurements at $LT < 1800$ ($Kp = 6^+$ and 8^-) are consistent with the fit obtained from measurements at later local times. We shall return to this point in the next section where it is suggested that, despite the arguments presented here, the data for large Kp are somewhat better approximated by (11) than by (4). The electric fields obtained from (4), (6), and (11) agree within a factor of 2 over the entire range $0 \leq Kp \leq 5$. For $Kp \leq 4.5$, the electric fields of (6) and (11) are bounded by the values previously given by *Rycroft* [1971] and by *Rycroft and Thomas* [1970].

COMPARISON WITH LOW-ALTITUDE MEASUREMENTS

The values of the electric fields found in (4), (6), (11) and (13) can be compared with *Heppner*'s [1972] measurements of polar cap electric fields. Heppner found that the integrated potential drop across the polar cap ranged from 20 to 100 kV, with typical values for moderate Kp, near 3, falling in the range 40–70 kV. For comparison, the potential drops across an assumed 40-R_E magnetosphere predicted from the equations mentioned are tabulated for several values of Kp in Table 1. The predictions of (11) appear most closely consistent with Heppner's measurements. Equation (6) gives values too large for small Kp and too small for large Kp.

TABLE 1. Total Dawn-Dusk Potential Drop in Kilovolts Predicted Across a 40-R_E Magnetosphere versus K_p

	K_p			
Equation No.	0	2	4	6
4	19	27	42	74
6	28	44	54	64
11	18	27	47	101
13	16	23	36	66
15	32	74	116	160

COMPARISON WITH IONOSPHERIC MEASUREMENTS

The position of the auroral oval is known to shift equatorward with increase of geomagnetic activity [*Feldstein*, 1974]. Equatorward displacement of the ionospheric boundary may be interpreted as the signature of inward convection of the plasma sheet in the equatorial plane, for the inner edge of the plasma sheet has been found to coincide with the equatorward edge of the auroral oval [*Vasyliunas*, 1970*b*; *Lassen*, 1974]. The convection model can then be invoked to provide an estimate of the equatorial electric field based on the auroral zone measurements.

The linear fit to the Kp dependence of the magnetic latitude (λ_M) of the equatorward boundary of the auroral oval shown by *Feldstein and Starkov* [1967] satisfies

$$\lambda_M = 65.2° - 1.04°Kp \qquad (14)$$

in the vicinity of local midnight. To map this to the equator, we note that in the Olson-Pfitzer model, the ATS field line ($L = 6.6$) at quiet time maps to approximately 65.2° magnetic latitude [*Olson and Pfitzer*, 1974]. An estimate of the equatorial L value L_A corresponding to the midnight auroral boundary is obtained by normalizing the dipole mapping so that it corresponds to the Olson-Pfitzer model when $Kp = 0$. It follows that

$$L_A = 1.16/[\cos^2(65.2° - 1.04°Kp)] \qquad (15)$$

If this boundary is also the inner edge of the plasma sheet, the strength of the electric field can be determined from the convection model. In this model, near the midnight meridian, electron convection boundaries lie at greater radial distances for more energetic particles [*Schield*, 1969]. The inner edge of the plasma sheet should thus correspond to the convection boundary evaluated for the low-energy end of the range of electron energies found in the plasma sheet (100 eV to 10 keV) [*Vasyliunas*, 1970*b*]. For these 100-eV electrons the correction to the zero energy solution is negligible [*Kivelson and Southwood*, 1975], so (2) may be used to give

$$E = \frac{22.5}{L_A^{\,2}} = 16.7 \cos^4(65.2° - 1.04°Kp) \ \frac{kV}{R_E} \qquad (16)$$

and this is plotted in Figure 4. For small values of Kp the correspondence with the results obtained directly from equatorial observations (equation (11)) is close. For large values of Kp the mapping of field lines to the equator is not realistic, and the discrepancies are not surprising.

Direct measurements of the electric field between 0100 and 0600 LT in the auroral ionosphere have shown that though the magnitude of the field increases with Kp, local turbulent variations of the field dominate the weak effect [*Mozer and Lucht*, 1974]. The ambiguities involved in mapping electric fields between the equator and the auroral zone (discussed by *Mozer*

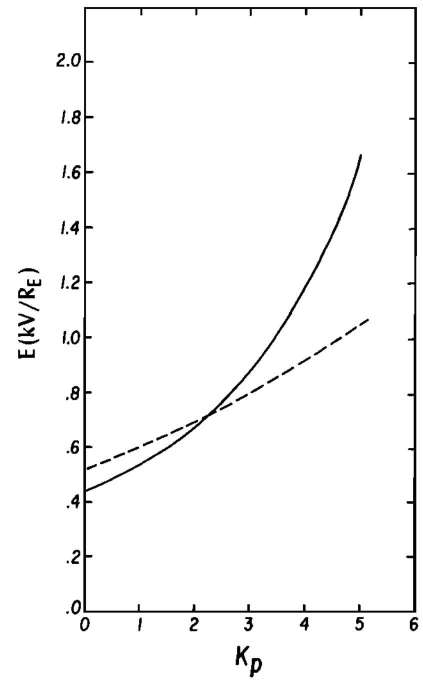

Fig. 4. Convection electric field versus *Kp*. Solid curve, empirical equation (11) from injection boundaries by *Mauk and McIlwain* [1974]. Dashed curve from the equatorward boundary of the auroral oval [*Feldstein and Starkov,* 1967] mapped to the equatorial plane using (16).

and Lucht [1974]) limit the value of detailed intercomparisons, but typical values of quiet time auroral zone fields mapped to the equator exceed the values obtained by other means by factors of 5–10. This overestimate probably reflects the important contribution to auroral zone measurements of localized turbulent fields which are superimposed on the large scale convection field [*Mozer and Manka,* 1971; *Mozer et al.,* 1974].

STORM TIME COMPARISONS

Observations of plasmapause erosion near local noon during the geomagnetic storm period, August 4–6, 1972, have been described by *Hoffman et al.* [1975]. These observations provide a useful test of the empirical expression of this paper, both because they apply to the predictions at very large *Kp*, and because they were made at local times excluded in the measurements used to establish the relation. Table 2 gives the observed parameters of the plasmapause, the convection field strength required to place the plasmapause at the observed location (equation (2)), the mean 3-hour *Kp* in the previous 24 hours, and the field strength calculated for this average *Kp* from (4) and (11). The empirical relations and the values inferred from observations are plotted in Figure 5. On one orbit the plasmapause lay inside perigee, so only a lower limit for the field is indicated in the table and on the figure. Once again, the agreement with both (4) and (11) is good, even at very disturbed times. Equation (6), obtained from the results of *Rycroft and Thomas* [1970], is also plotted in Figure 5 and, as in the previous comparison with polar cap potential drops, appears to underestimate the field for high values of *Kp*.

One point should be made regarding the values of *Kp* used in the above analysis. It has been noted that *Carpenter* [1967] associated the dawn plasmapause with the largest *Kp* observed in the previous 24 hours because this improved the correlation. *Mauk and McIlwain* [1974], on the other hand, used *Kp* interpolated to the encounter time and found a worse fit if they used *Kp* for 2 hours postencounter, whereas *Kp* of the 2-hour preencounter time enhanced the scatter somewhat near dusk but improved it slightly in the postmidnight region. These features can be interpreted in terms of the assumed model. If E increases when *Kp* increases, convection begins immediately; thus freshly accelerated particles appear at the Alfvén layer in the evening quadrant with delays of less than 2 hours, as observed by *Mauk and McIlwain* [1974] and *Freeman* [1974]. On the other hand, adjustment of the plasmapause to an enhanced electric field can take a full day, for the plasma which lies between the old and new Alfvén layers must drift around to the day side before the newly established open drift paths diverge from the initial closed orbits. Only after a full day will all flux tubes have convected to the day side, and thus the new boundaries will be established. At the dawn plasmapause the new equilibrium should occur with a delay of more than 12 hours, which accounts for Carpenter's result. Plasma convecting to the day side, having been present in the critical

TABLE 2. Explorer 45 Plasmapause Observations, August 2–4, 1972

Orbit	LT	L_{pp}	E	E_4	E_{11}	$\langle Kp \rangle$
818	13.84	4.6	1.4	0.56	0.56	1.2
819	13.02	4.2	1.5	0.78	0.83	2.8
820	12.04	3.5	1.8	1.1	1.3	4.3
821	12.04	3.1	2.4	1.4	1.8	5.2
822	11.31	2.8	3.0	2.2	3.4	6.6
823	10.19	2.3	3.5	2.5	4.3	7.0
824	···	<2.1	>4.2	3.9	8.8	8.0
825	10.42	2.2	3.7	3.0	5.5	7.4
826	9.82	2.2	3.7	2.5	4.3	7.0
827	10.88	2.6	3.0	1.9	2.8	6.2
828	12.64	3.8	1.7	1.5	2.0	5.5

Observations were by *Hoffman et al.* [1975]; L_{pp} is measured distance to plasmapause at the local time indicated, E is inferred from (2), $\langle Kp \rangle$ is the average 3-hour *Kp* for the previous 24 hours, E_4 and E_{11} are obtained from $\langle Kp \rangle$ and (4) and (11), respectively.

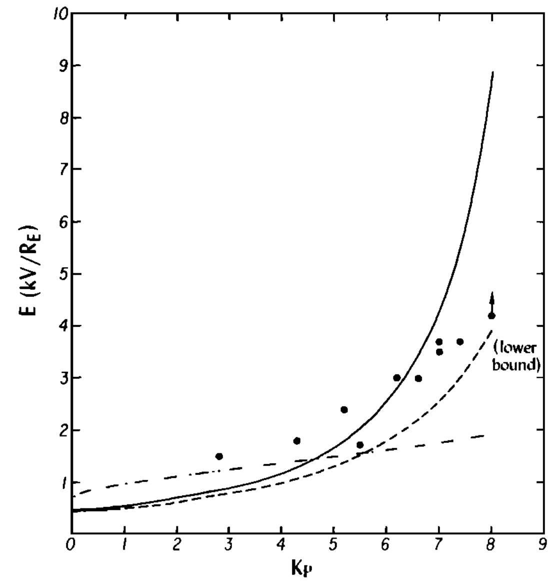

Fig. 5. Magnitude of a uniform dawn-dusk electric field versus *Kp* for very disturbed times. The solid curve represents (11), the dashed curve (4), and the dotted and dashed curve (6) [*Rycroft and Thomas,* 1970]. The dots are obtained from Explorer 45 observations of plasmapause erosion during a magnetic storm [*Hoffman et al.,* 1975].

flow region for most of a day, should be best characterized by some long-time average of the geomagnetic conditions, and hence we have used the stated 24-hour average *Kp*.

RELATION OF OTHER MODELS OF THE ELECTRIC FIELD

Analytic models of the convection electric field somewhat more complex than the uniform dawn-dusk field have been developed in recent years [*Volland*, 1973; *Stern*, 1975], and if the *Kp*-dependent particle boundaries were interpreted in terms of these models, the empirical relations between *Kp* and field strength would be somewhat different. As a more complex model field varies in space, its magnitude must be characterized by some average value such as the total potential drop across the 30-R_E width of the magnetosphere in the dawn-dusk meridian.

A simplified version of *Volland*'s [1973] field, attributed to Stern, is used by *Maynard and Chen* [1975]. This Volland-Stern-Maynard-Chen (VSMC) field is symmetric about the dawn-dusk meridian, and its amplitude increases with *Kp*; the Alfvén layer for $Kp = 3.7$ is illustrated in Figure 6. Also shown is the Alfvén boundary for the uniform field corresponding to $Kp = 3.7$ in (11) and a portion of the orbit of a geostationary satellite. This diagram indicates that the field strengths obtained from the local time versus *Kp* fits of (8) and (9) would be only slightly modified by use of the VSMC model, and this point is confirmed by Figure 7, on which the filled circles were evaluated from the VSMC model by a procedure analogous to that used to derive (11). Numbers in parentheses show the percent deviation of the electric field values from the curve (equation (11)) and are seen to be of the order of 30%. The large separation near dawn of the Alfvén boundaries of the uniform and VSMC models seen in Figure 6 suggests that discrepancies between the models may increase postmidnight. For example, in the VSMC model the dawn plasmapause never moves inside $L = 4$, clearly at variance with *Carpenter*'s [1967] observations. Consequently, the model does not produce self-consistent relations between field strength and *Kp* when used to interpret observations in different time intervals. For these reasons we have preferred to use the uniform field model, which seems reasonably consistent with most observations except very near the dusk meridian.

Other field models which have been given by *Volland* [1973] and *McIlwain* [1974] are illustrated in Figures 8 and 9, and on

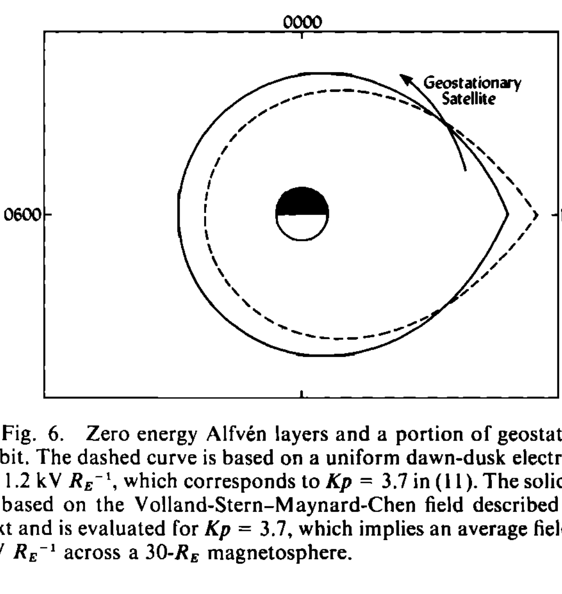

Fig. 6. Zero energy Alfvén layers and a portion of geostationary orbit. The dashed curve is based on a uniform dawn-dusk electric field of 1.2 kV R_E^{-1}, which corresponds to $Kp = 3.7$ in (11). The solid curve is based on the Volland-Stern-Maynard-Chen field described in the text and is evaluated for $Kp = 3.7$, which implies an average field of 39 kV R_E^{-1} across a 30-R_E magnetosphere.

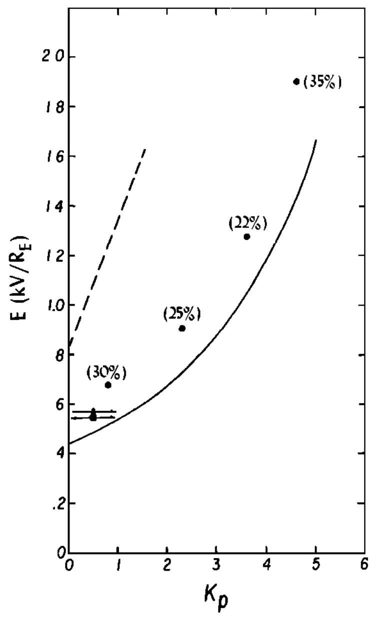

Fig. 7. Convection electric field versus *Kp*. Solid curve, (11). Filled circles inferred from ATS 5 injection boundaries of *Mauk and McIlwain* [1974] and the Volland-Stern-Maynard-Chen electric field model described in the text. The diamond indicates the average electric field across 30 R_E in the dawn-dusk meridian for the *Volland* [1973] quiet time (Kp = 0–1) model; the square indicates the same quantity for the *McIlwain* [1974] EH3 model. Numbers in parentheses are the percent disagreement of the fields based on the two models. Dashed curve is the fit of *Chen and Grebowsky* [1974] given in (17).

Figure 7 two points are included showing the average field strength of the McIlwain model and of the Volland 'quiet' model, both based on data for a *Kp* range from 0–1. The points fall close to the curve representing (11). Volland's 'disturbed' field, said to apply for *Kp* in the range 2–4, corresponds to an average electric field of 2.2 kV/R_E, which is much larger than the values given by (11). Note in Figure 8 that Volland's 'disturbed' field places the plasmapause near dawn at $L = 3.3$, i.e., at a distance normally expected for $Kp = 5$. The suggestion therefore is that the 'disturbed' field may be better assigned to the range 4–6 for *Kp*, which would bring its average magnitude into the range of the predictions of (11).

A linear relation between *E* and *Kp* used by *Chen and Grebowsky* [1974]

$$E = 0.795(1 + \tfrac{2}{3}Kp) \quad \text{kV}/R_E \qquad (17)$$

also plotted in Figure 7, seems to overestimate the field strength for all *Kp*.

Roederer and Hones [1974] have developed a model time-dependent electric field to describe the injection of particles at geostationary orbit during substorms. In their model the potential drop across 20 R_E in the dawn-dusk meridian plane increases linearly for 10 min from 0 to 60 kV, then decreases linearly to 0 in 120 min. The average electric field across the dawn-dusk meridian during the 130-min interval containing the model substorm is 1.5 kV/R_E, while for a full 3-hour interval spanning an isolated model substorm the average electric field is 1.1 kV/R_E. For $E = 1.1$ kV/R_E, (11) gives $Kp = 4^-$, a value which is frequently regarded as 'moderately disturbed.' The Roederer-Hones isolated substorm electric field is therefore in reasonable agreement with (11).

Kuznetsov [1972] has obtained a linear relation between *E* and *Kp* by examination of morning-evening asymmetries of

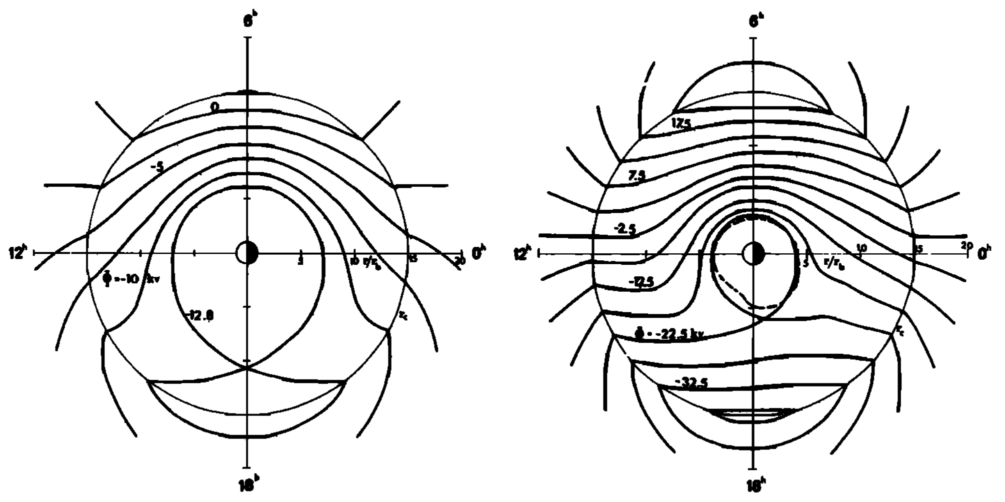

Fig. 8. *Volland*'s [1973] equatorial electric field equipotentials, including the corotation field. On the left is the quiet time (Kp = 0–1) model. On the right is the disturbed (Kp = 2–4) model which, as described in the text, may be more correctly associated with Kp = 4–6.

the flux of >35-keV outer belt electrons. The innermost L shell on which asymmetry is detected (L_K) is found to move earthward with increasing Kp. Attributing the asymmetry to the presence of newly accelerated plasma sheet electrons on the morning side, Kuznetsov interprets L_K as the boundary between open and closed drift orbits for energetic electrons. The arguments are similar to those used to obtain (11), but as the boundary for 35-keV electrons lies well outside the boundaries for low-energy electrons, his analysis is more sensitive to departures from the dipole magnetic field used in both cases to interpret the data. Furthermore, the acceleration of particles by the strongly time-dependent magnetic fields which frequently occur near midnight during substorms will systematically increase the electric fields inferred from the morning-evening asymmetries. Nonetheless, the relation obtained by *Kuznetsov* [1972]

$$E = 0.87(1 + 0.71Kp) \quad \text{kV}/R_E \qquad (18)$$

differs from (11) only by a factor of <3.2 in the range Kp from 0 to 8.

Finally, a comparison with the pioneer relation between E and Kp [*Vasyliunas,* 1968] should be made. Vasyliunas obtained his expression

$$E = (2.55 \text{ kV}/R_E)/(1 - 0.1Kp)^2 \qquad (19)$$

by relating the distance to the dusk stagnation point in a uniform field model to the electric field, but for the distance to the stagnation point, he used *Binsack*'s [1967] measurements of the distance to the plasmapause averaged over all local times ($L = 6 - 0.6Kp$). The asymmetry of the Alfvén layers illustrated in Figure 3 shows that this procedure seriously underestimates the distance to the stagnation point. Indeed, Binsack's expression is identical with the *Carpenter and Park* [1973] expression for the distance to the dawn plasmapause to one significant figure. On the other hand, in the uniform field model the ratio of the distances to the plasmapause at dawn and dusk is 0.4. As E varies as the inverse square of the distance to the stagnation point, (19) should be modified by multiplying it by $(0.4)^2$, and it would then be approximately the same as (4). (This argument has been given in an unpublished document: A. J. Chen, personal communication, 1975).

APPLICATIONS

From the injection boundaries described by (9), *Freeman* [1974] inferred the radial distance at midnight to the inner boundary of convection (inner edge of the plasma sheet) by assuming that the particles forming the ATS 1 injection boundary included only particles of magnetic moment μ and greater. His results, based on the electric field of *Vasyliunas* [1968], given here as (19), indicated that electrons of a wide range of magnetic moments could penetrate to geostationary orbit at midnight for moderately disturbed geomagnetic conditions.

We have reexamined the midnight plasma sheet boundary, assuming from the injection spectra used by *Mauk and McIlwain* [1974] that the injected particles have magnetic moments of ≥0 and that consequently the plasma sheet at midnight is composed of particles convected in as far as their Alfvén

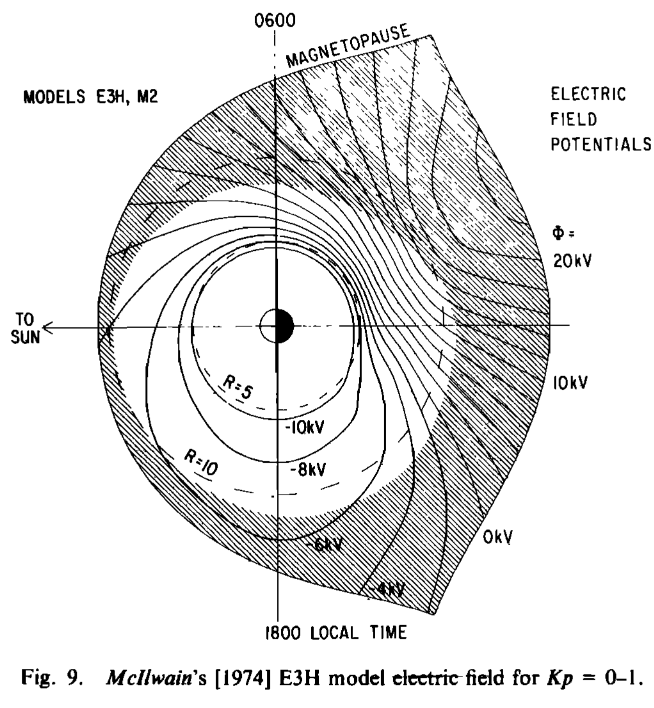

Fig. 9. *McIlwain*'s [1974] E3H model ~~electric field~~ for Kp = 0–1.

boundaries. We have used the approximations for finite μ electrons given by *Kivelson and Southwood* [1975] and have included corotation fields. At midnight for electrons of 90° pitch angle and sufficiently large μ, the distance to the Alfvén boundary L_M satisfies

$$eER_E = \frac{0.47B_0\mu}{L_M^4} + \frac{21}{L_M^2} \quad (20)$$

where the particle kinetic energy is $\mu B_0/L^3$ in keV. (The coefficients differ slightly when μ is very small.) Values of L_M for small μ and a range of Kp are given in Table 3, from which it is clear that only particles with extremely small magnetic moments can reach geostationary orbit at midnight for Kp = 2. The difference between our conclusion and Freeman's is due to the much smaller electric fields we have used.

An estimate of the dependence of the dawn-dusk electric field on the solar wind velocity (V_{sw}), analogous to those given by *Vasyliunas* [1968] and *Mendillo and Papagiannis* [1971], can be found from (4) and the relation between V_{sw} and Kp obtained by *Snyder et al.* [1963], which, if expressed in terms of the average 3-hour Kp in the previous 24 hours, is approximately

$$V_{sw} \text{ km/s} = 68Kp + 330 \quad (21)$$

From (19) and (11) it follows that

$$E = \frac{0.2 \text{ kV } R_E^{-1}}{[(1 - V_{sw} \text{ km/s})/1000]^2} \quad (22)$$

The validity, even in a statistical sense, of (22) is restricted to the range of solar wind velocities which Snyder et al. used to establish (21). In their work, 330 km/s < V_{sw} < 750 km/s, and the average value was V_{sw} = 504 km/s. Obviously then, one should conclude neither that a convection electric field exists in the absence of a solar wind nor that the electric field becomes infinite at V_{sw} = 1000 km/s. It is worth noting that (22) corresponds quite closely to a one-parameter quadratic form ($E = 3.2 (V_{sw}/100)^2$ kV/R_E), selected to give agreement for the average solar wind velocity previously cited, and diverges considerably from an analogously chosen linear form ($E = 1.6 (V_{sw}/1000)$). This observation supports the theoretical conclusion of *Mendillo and Papagiannis* [1971] that the convection electric field varies more nearly quadratically than linearly with the solar wind velocity.

From (22), one can estimate the size of the day side 'merging' region required to account for the convection field, again limiting applications to 330 km/s ≤ V_{sw} ≲ 750 km/s. For a solar wind magnetic field of ~5 γ, with a component of the order of 3 γ parallel to the earth's dipole, the width of the merging region (Δy) across the day side scales as

$$\Delta y\ (R_E) \sim \frac{0.4}{(V_{sw}/1000)(1 - V_{sw}/1000)^2} \quad (23)$$

which for V_{sw} = 500 gives ~3 R_E for the width of the merging region.

TABLE 3. Distances in Earth Radii to the Alfvén Layers on the Midnight Meridian for Electrons of Magnetic Moment μ for different Kp

	Kp					
μ, keV/γ	0	1	2	3	4	5
0	7.5	6.7	5.7	5.0	4.3	3.8
0.05	8.7	8.0	7.1	6.5	5.9	5.3
0.1	9.6	8.8	7.9	7.3	6.6	6.1
0.16	10.3	9.6	8.6	7.9	7.3	6.7

Kp = 0 LIMIT

The empirical relation between E and Kp (equation (11)) has a nonzero limit for $Kp \to 0$, and if this limit is not spurious, it is physically interesting, for it suggests the presence of an electric field in the absence of any other significant geomagnetic activity. However, the position of the plasmapause, which we have used to determine the field, cannot be observed at times of prolonged quiet conditions as it becomes exceedingly ill defined [*Chappell et al.*, 1970*a*]. If particle injections occur for Kp = 0, we are more likely to conclude that the Kp index is not a good measure of the level of activity than to believe that we have learned something about convection fields. Unfortunately, present data are insufficient to test the significance of the limiting value of the convection electric field.

SUMMARY

The empirical expression (equation (11)) E (kV/R_E) = $0.44/(1 - 0.097Kp)^2$ accords well with observations of the dependence on Kp of the average positions of diverse particle boundaries in the magnetosphere and with measured polar cap electric fields for 0 ≤ Kp ≲ 8. This relation, which is approximately the same as those given in (4) and (13), has been favored primarily because it agrees somewhat better with polar cap field measurements and because it predicts storm time locations of the plasmapause quite well.

Naturally, the uniform field model must be used with care. For example, the position of the Alfvén boundary in the electric field given by (11) is not expected to correspond to a clearly defined gradient in the plasma density during intervals of decreasing magnetic activity when flux tubes, empty because they lie outside a previous Alfvén layer, have not yet regained equilibrium with the ionosphere. Similarly, because of the absence of a sharp gradient at the plasmapause at low Kp [*Chappell et al.*, 1970*a*], the position of the boundary depends sensitively on the criterion used to define it (e.g., density greater than 10 cm^{-3} or 100 cm^{-3}), and this dependence on an arbitrary criterion can present problems for analysis of quiet time properties.

Although a relation between the convection field and Kp can be valid at best only in a statistical sense, it should be useful for calculating the expected drift paths of particles during magnetically active times. Equation (11) may, for example, be applied to further analysis of the redistribution of low-energy plasma during geomagnetically active times of the type initiated by *Chen and Grebowsky* [1974, and references therein]. In addition, the behavior of particles of nonzero energy, which are also affected by convection electric fields, can be studied by using the estimated fields. The variation in the field amplitude as Kp changes may also provide an estimate of the power in low-frequency electric field variations which may be of use in studies of radial diffusion [*Fälthammar*, 1968]. However, as Kp is itself averaged over both time and space, it can at best characterize only large scale activity and time-averaged behavior. Accordingly, the electric fields associated with Kp in the results of this paper should be applied to the analysis of time-averaged large scale behavior only.

Acknowledgments. Stimulating discussions with C. T. Russell are gratefully acknowledged. This work was supported by NSF through grant DES 74-23464. This article is Institute of Geophysics and Planetary Physics publication 1478-82.

REFERENCES

Alfvén, H., and C.-G. Fälthammar, *Cosmical Electrodynamics*, Oxford University Press, London, 1963.

Axford, W. I., Magnetospheric convection, *Rev. Geophys. Space Phys., 7*, 421, 1969.

Bezrukikh, V. V., Results of measurements of charged particle density on board Electron-2 and Electron-4 within the earth's plasma sheath (in Russian), *Kosm. Issled., 8*, 273, 1970. (*Cosmic Res., 8*, 251, 1970.)

Binsack, J. H., Plasmapause observations with the MIT experiment on Imp 2, *J. Geophys. Res., 72*, 5231, 1967.

Brice, N. M., Bulk motion of the magnetosphere, *J. Geophys. Res., 72*, 5193, 1967.

Carpenter, D. L., Relations between the dawn minimum in the equatorial radius of the plasmapause and *Dst*, *Kp*, and local *K* at Byrd Station, *J. Geophys. Res., 72*, 2969, 1967.

Carpenter, D. L., and C. G. Park, On what ionospheric workers should know about the plasmapause-plasmasphere, *Rev. Geophys. Space Phys., 11*, 133, 1973.

Chappell, C. R., The convergence of fact and theory on magnetospheric convection, in *Correlated Interplanetary and Magnetospheric Observations*, edited by D. E. Page, D. Reidel, Dordrecht, Netherlands, 1974.

Chappell, C. R., K. K. Harris, and G. W. Sharp, A study of the influence of magnetic activity on the location of the plasmapause as measured by Ogo 5, *J. Geophys. Res., 75*, 50, 1970*a*.

Chappell, C. R., K. K. Harris, and G. W. Sharp, The morphology of the bulge region of the plasmasphere, *J. Geophys. Res., 75*, 3848, 1970*b*.

Chen, A. J., Penetration of low-energy protons deep into the magnetosphere, *J. Geophys. Res., 75*, 2458, 1970.

Chen, A. J., and J. M. Grebowsky, Plasma tail interpretations of pronounced detached plasma regions measured by Ogo 5, *J. Geophys. Res., 79*, 3851, 1974.

Fälthammar, C.-G., Coefficients of diffusion in the outer radiation belt, in *Radiation Trapped in the Earth's Magnetic Field*, edited by B. M. McCormac, p. 157, Reinhold, New York, 1968.

Feldstein, Y. I., Auroras and associated phenomena, in *Solar Terrestrial Physics, 3*, edited by E. R. Dyer, D. Reidel, Dordrecht, Netherlands, 1972.

Feldstein, Y. I., Night-time aurora and its relation to the magnetosphere, *Ann. Geophys., 30*, 259, 1974.

Feldstein, Y. I., and G. V. Starkov, Dynamics of auroral belt and polar geomagnetic disturbances, *Planet. Space Sci., 15*, 209, 1967.

Freeman, J. W., *Kp* dependence of the plasma sheet boundary, *J. Geophys. Res., 79*, 4315, 1974.

Gringauz, K. I., Low-energy plasma in the magnetosphere, *Rev. Geophys. Space Phys., 7*, 339, 1969.

Heppner, J. P., Electric field variations during substorms, *Planet. Space Sci., 20*, 1475, 1972.

Hoffman, R. A., et al., Explorer 45 (S^3-A) observations of the magnetosphere and magnetopause during the August 4–6, 1972, magnetic storm period, *J. Geophys. Res., 80*, 4287, 1975.

Kavanagh, L. D., Jr., J. W. Freeman, Jr., and A. J. Chen, Plasma flow in the magnetosphere, *J. Geophys. Res., 73*, 5511, 1968.

Kivelson, M. G., and D. J. Southwood, Approximations for the study of drift boundaries in the magnetosphere, *J. Geophys. Res., 80*, 3528, 1975.

Kuznetsov, S. N., Estimate of electric fields in the earth's magnetosphere (in Russian), *Geomagn. Aeron., 12*, 354, 1972.

Lassen, K., Relation of the plasma sheet to the nighttime auroral oval, *J. Geophys. Res., 79*, 3857, 1974.

Mauk, B. H., and C. E. McIlwain, Correlation of *Kp* with the substorm-injected plasma boundary, *J. Geophys. Res., 79*, 3193, 1974.

Maynard, N. C., and A J. Chen, Isolated cold plasma regions: Observations and their relation to possible production mechanisms, *J. Geophys. Res., 80*, 1009, 1975.

McIlwain, C. E., Substorm injection boundaries, in *Magnetospheric Physics*, edited by B. M. McCormac, D. Reidel, Dordrecht, Netherlands, 1974.

Mendillo, M., and M. D. Papagiannis, Estimate of the dependence of the magnetospheric electric field on the velocity of the solar wind, *J. Geophys. Res., 76*, 6939, 1971.

Mozer, F. S., Origin and effects of electric fields during isolated magnetospheric substorms, *J. Geophys. Res., 76*, 7595, 1971.

Mozer, F. S., and P. Lucht, The average auroral zone electric field, *J. Geophys. Res., 79*, 1001, 1974.

Mozer, F. S., and R. H. Manka, Magnetospheric electric field properties deduced from simultaneous balloon flights, *J. Geophys. Res., 76*, 1697, 1971.

Mozer, F. S., R. Serlin, D. L. Carpenter, and J. Siren, Simultaneous electric field measurements near $L = 4$ from conjugate balloons and whistlers, *J. Geophys. Res., 79*, 3215, 1974.

Nishida, A., Formation of plasmapause, or magnetospheric plasma knee, by the combined action of magnetosphere convection and plasma escape from the tail, *J. Geophys. Res., 71*, 5669, 1966.

Olson, W. P., and K. A. Pfitzer, A quantitative model of the magnetospheric magnetic field, *J. Geophys. Res., 79*, 3739, 1974.

Park, C. G., Whistler observations of the interchange of ionization between the ionosphere and the protonosphere, *J. Geophys. Res., 75*, 4249, 1970.

Roederer, J. G., and E. W. Hones, Jr., Motion of magnetospheric particle clouds in a time-dependent electric field model, *J. Geophys. Res., 79*, 1432, 1974.

Rycroft, M. J., Dawn-dusk electric fields across the magnetosphere derived from plasmapause observations, Proceedings of the Colloquium Wave-Particle Interactions in the Magnetosphere, pp. 163–170, *Rep. N72-15339*, U.S. Nat. Tech. Inform. Serv., Springfield, Va., 1971.

Rycroft, M. J., Magnetospheric plasma flow and electric fields derived from whistler observations (abstract), *Quart. J. Roy. Astron. Soc., 15*, 296, 1974.

Rycroft, M. J., A review of in situ observations of the plasmapause, *Ann. Geophys., 31*, 1, 1975.

Rycroft, M. J., and J. O. Thomas, The magnetospheric plasmapause and the electron density trough at Alouette 1 orbit, *Planet. Space Sci., 18*, 65, 1970.

Schatten, K. H., and J. M. Wilcox, Response of the geomagnetic activity index *Kp* to the interplanetary magnetic field, *J. Geophys. Res., 72*, 5185, 1967.

Schield, M. A., Drift of non-interacting charged particles in a simple geomagnetic field, *Rep. 69-54*, Univ. of Iowa, Iowa City, 1969.

Schield, M. A., J. W. Freeman, and A. J. Dessler, A source for field-aligned currents at auroral latitudes, *J. Geophys. Res., 74*, 247, 1969.

Snyder, C. W., M. Neugebauer, and U. R. Rao, The solar wind velocity and its correlation with cosmic ray variations and with solar and geomagnetic activity, *J. Geophys. Res., 68*, 6361, 1963.

Stern, D. P., Quantitative models of magnetic and electric fields in the magnetosphere, *NASA-GSFC Doc. X-602-75-90*, April 1975.

Taylor, H. A., Jr., H. C. Brinton, and M. W. Pharo III, Contraction of the plasmasphere during geomagnetically disturbed periods, *J. Geophys. Res., 73*, 961, 1968.

Vasyliunas, V. M., A crude estimate of the relation between the solar wind speed and the magnetospheric electric field, *J. Geophys. Res., 73*, 2529, 1968.

Vasyliunas, V. M., Mathematical models of magnetospheric convection and coupling to the ionosphere, in *Particles and Fields in the Magnetosphere*, edited by B. M. McCormac, p. 60, D. Reidel, Dordrecht, Netherlands, 1970*a*.

Vasyliunas, V. M., Low energy particle fluxes in the geomagnetic tail, in *Polar Ionosphere and Magnetospheric Processes*, edited by G. Skovli, Gordon and Breach, New York, 1970*b*.

Volland, H., A semiempirical model of large-scale magnetospheric electric fields, *J. Geophys. Res., 78, 171, 1973.*

Wilcox, J. M., K. Schatten, and N. Ness, Influence of interplanetary magnetic field and plasma on geomagnetic activity during quiet sun conditions, *J. Geophys. Res., 72*, 19, 1967.

Wolf, R. A., Effects of ionospheric conductivity on convective flow of plasma in the magnetosphere, *J. Geophys. Res., 75*, 4677, 1970.

(Received August 1, 1975;
accepted December 3, 1975.)